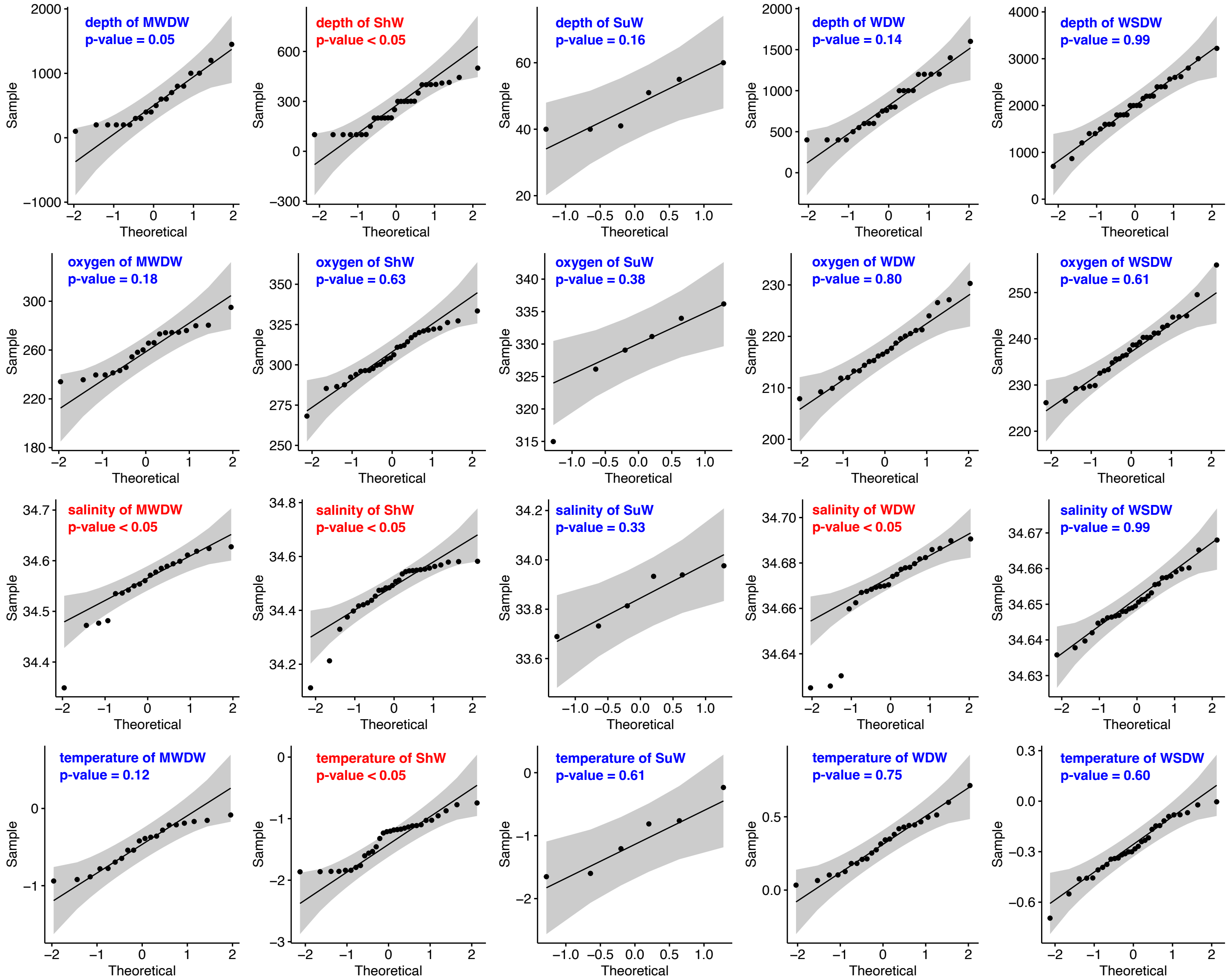


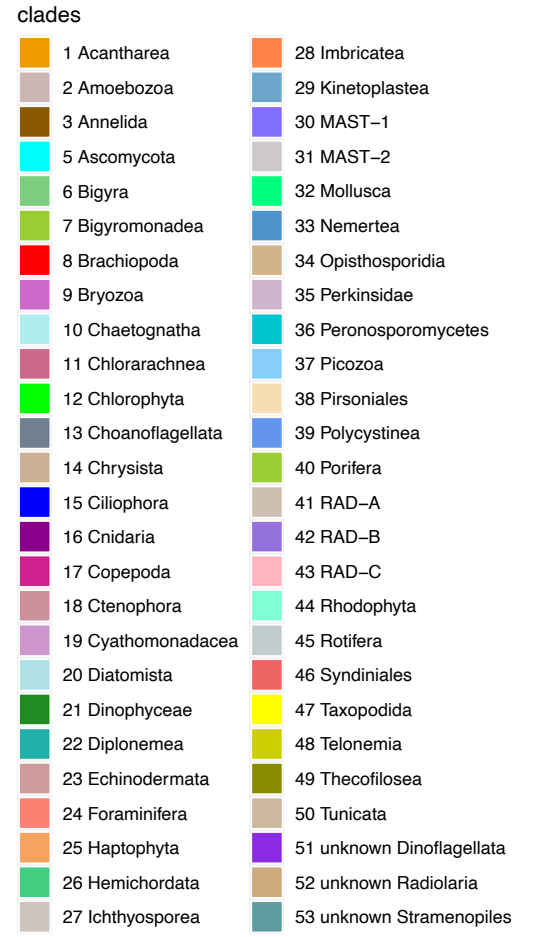
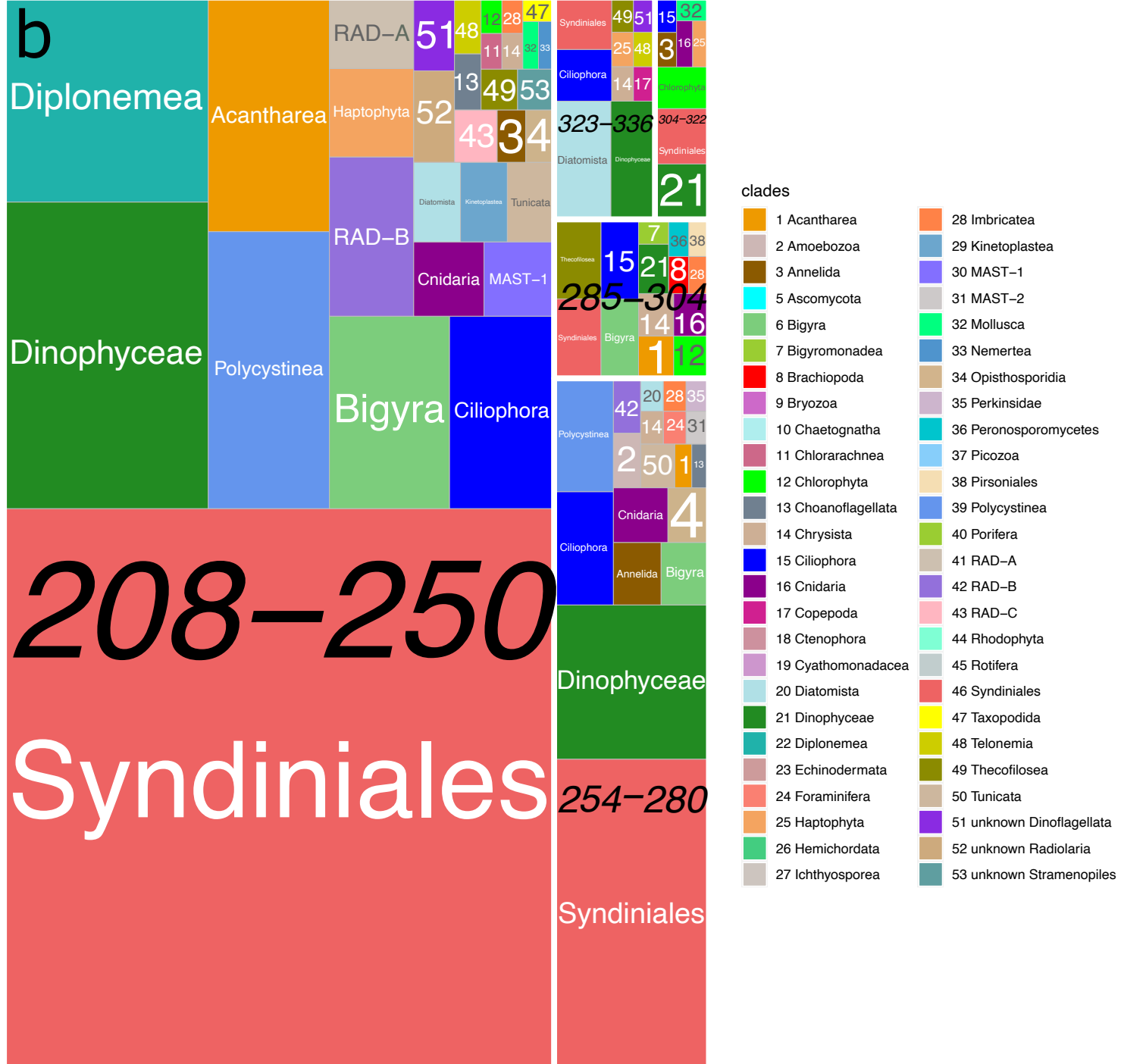
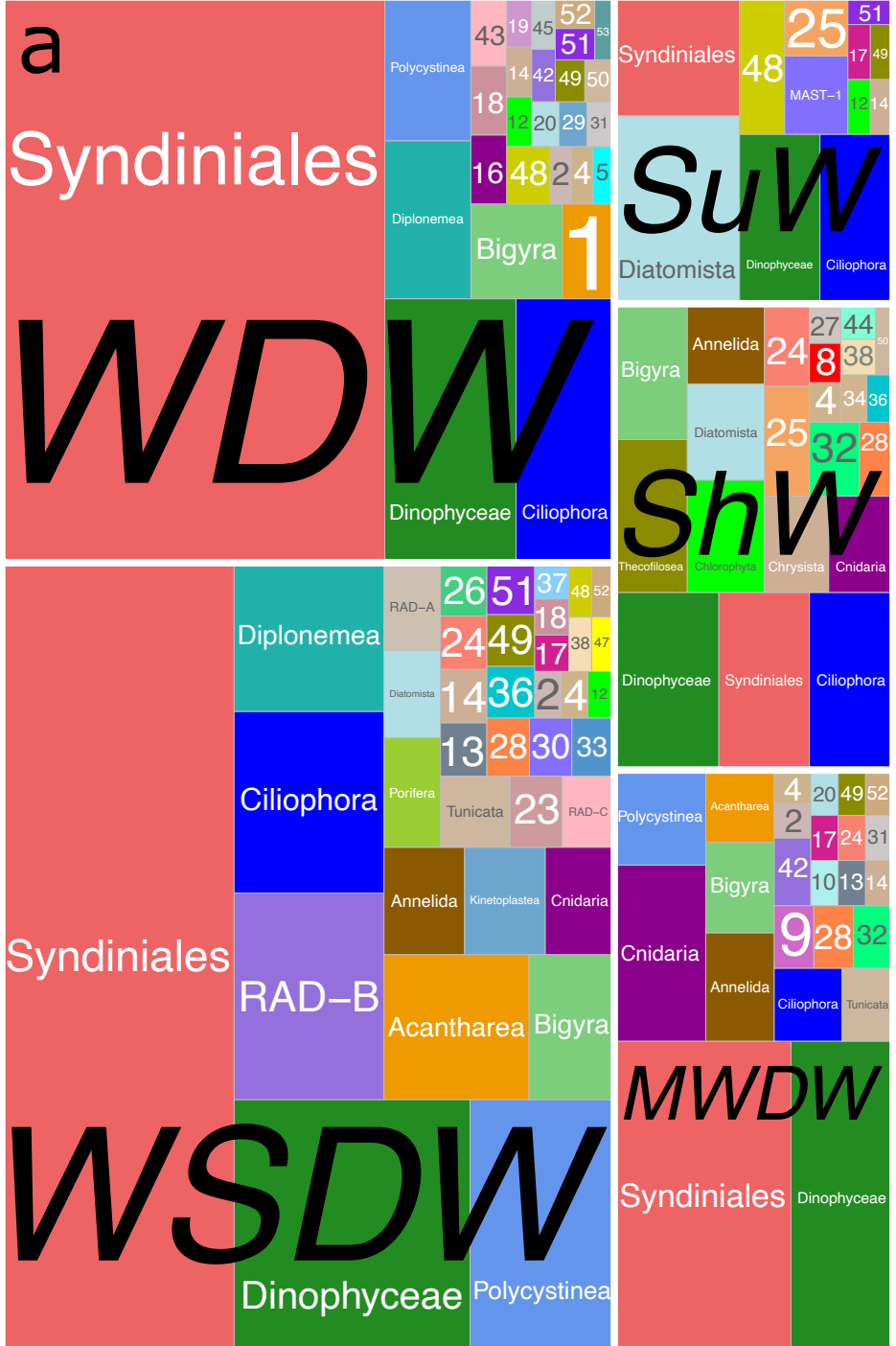
**Suppl. Fig. 1.** Two-dimensional NMDS plots illustrating pairwise Bray-Curtis distances between pico-nano eukaryotic communities in the Western Weddell Sea. All NMDS plots are identical (with a stress value = 0.075 is shown in panel **A**), but the samples are clustered in different ways as described below. The water masses are mapped on the NMDS plot in the upper left corner, along with the environmental variables measured in this study and geographical coordinates. Boundary points on gradients of those variables (where pico-nano eukaryotic community composition is significantly different across the boundary) were identified using a split moving-window analysis of ecological differentiation based on a Z-score cutoff of 1.2 , and samples were clustered according to these boundary points. The clusters are colored and marked with polygons. The intervals of the variable corresponding to the clusters are shown in the legends on top of each plot. Mantel correlation coefficients (calculated for a matrix of Bray-Curtis distances between the pico-nano eukaryotic communities and for a matrix of Bray-Curtis distances between the samples based on a variable) are shown for each continuous variable.



**Suppl. Fig. 2.** Normality test results for depth, oxygen concentration, salinity, and temperature across five water masses. Quantile-Quantile plots, confidence intervals and p-values of the Shapiro-Wilk test are shown.

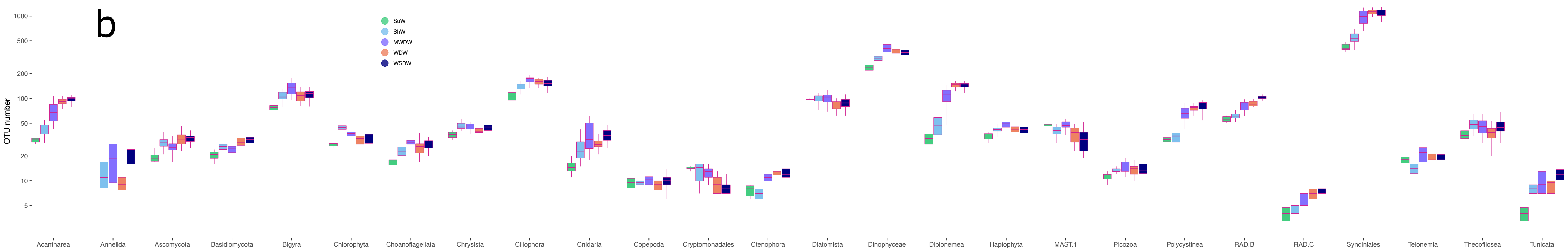
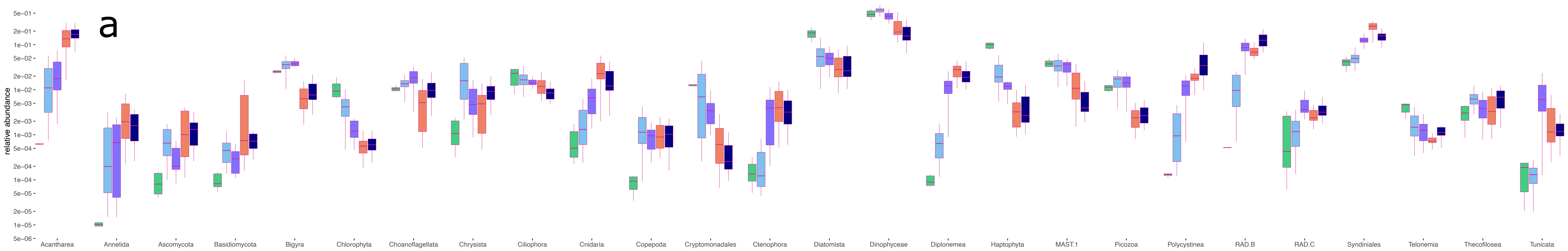


**Suppl. Fig. 3.** A summary of GAM results showing influence of abiotic variables on relative abundance or OTU richness of 26 eukaryotic clades. Percentages of variance explained by GAM models are shown for clade/variable pairs on the y-axis. The environmental variables are coded by color and grouped into four categories: depth, oxygen, salinity, and the other variables. For relative abundance or OTU richness of each clade, only the highest variance explained across all the environmental variables is shown, hence each clade appears in one category only.

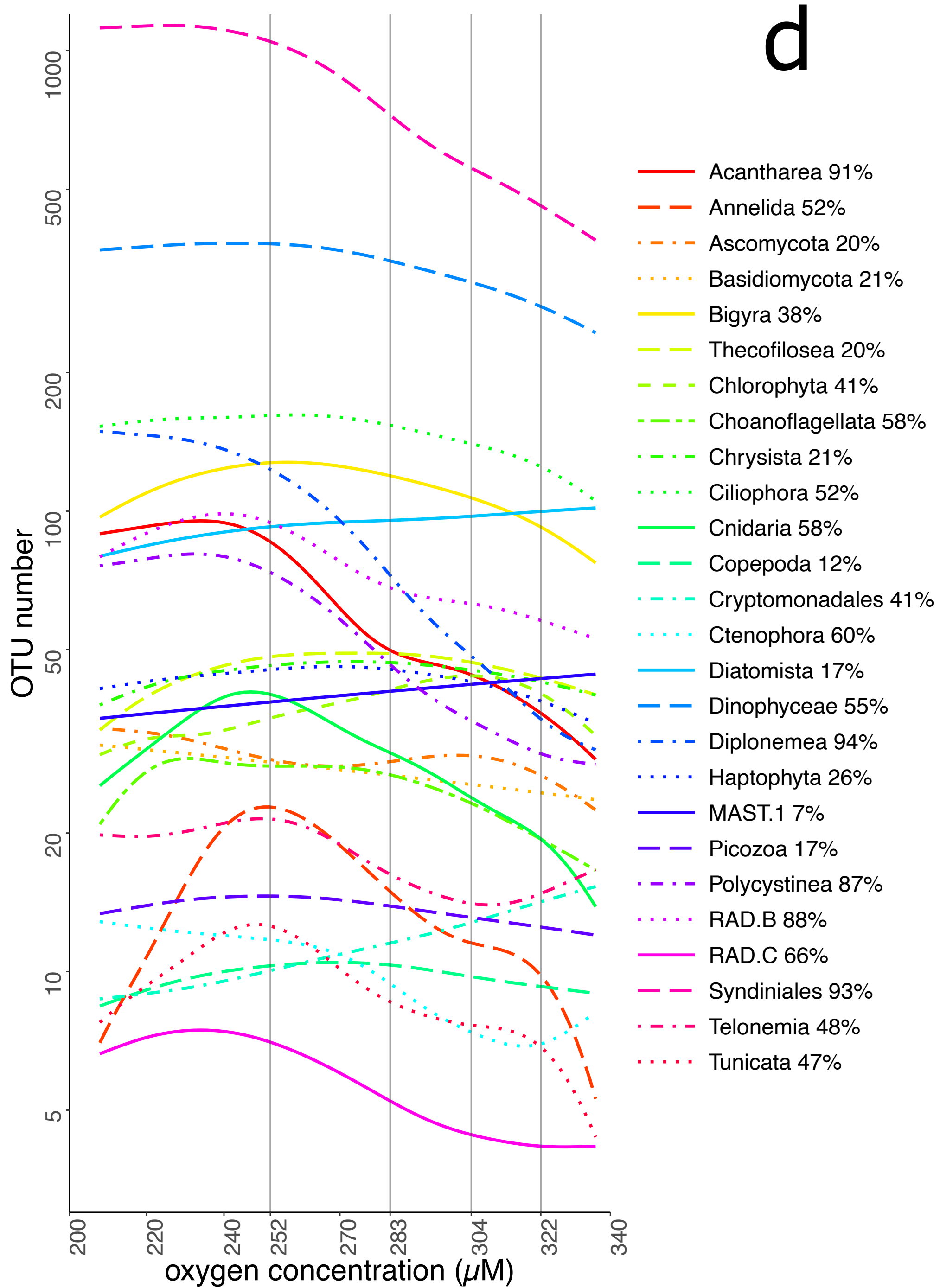
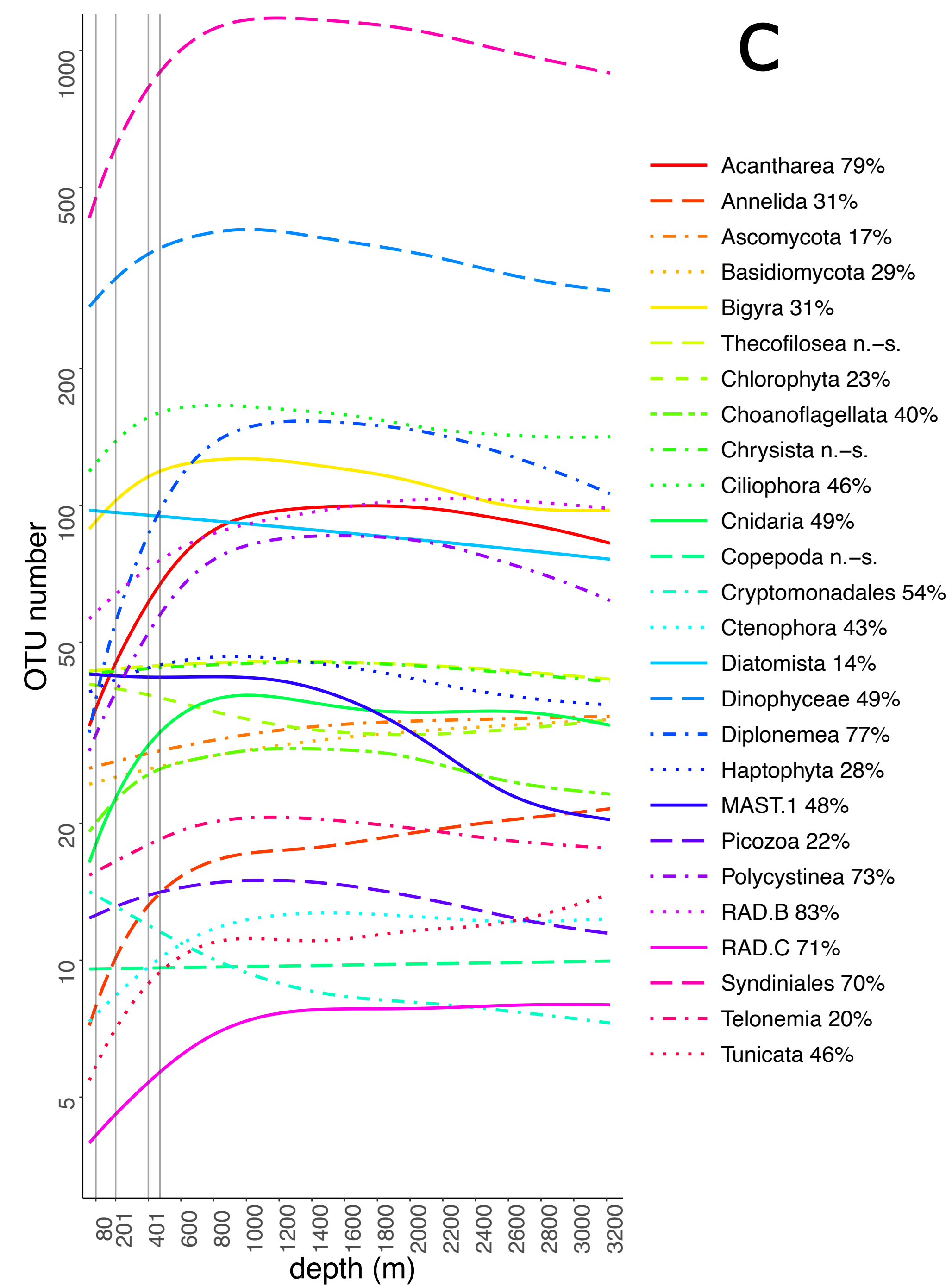
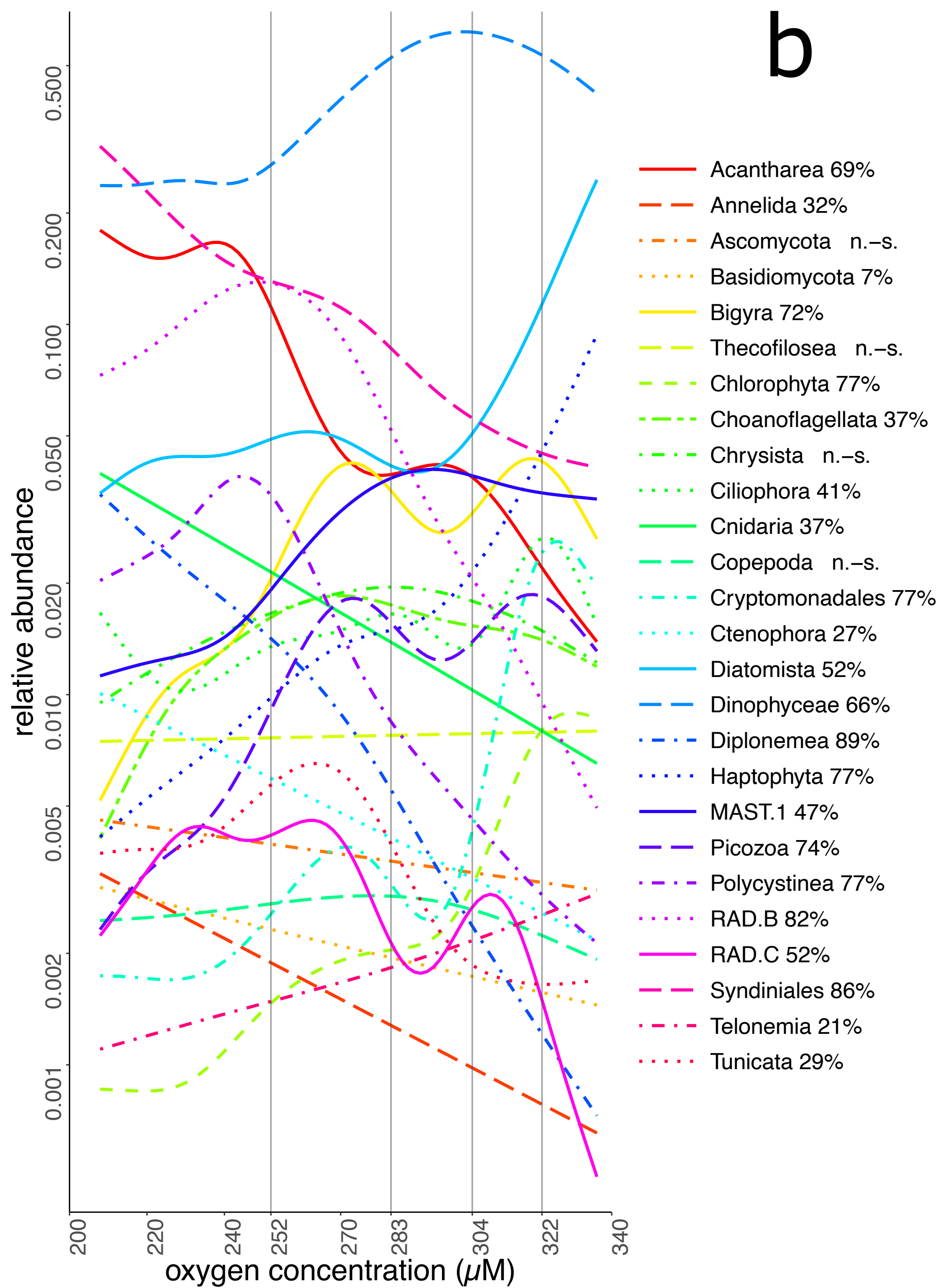
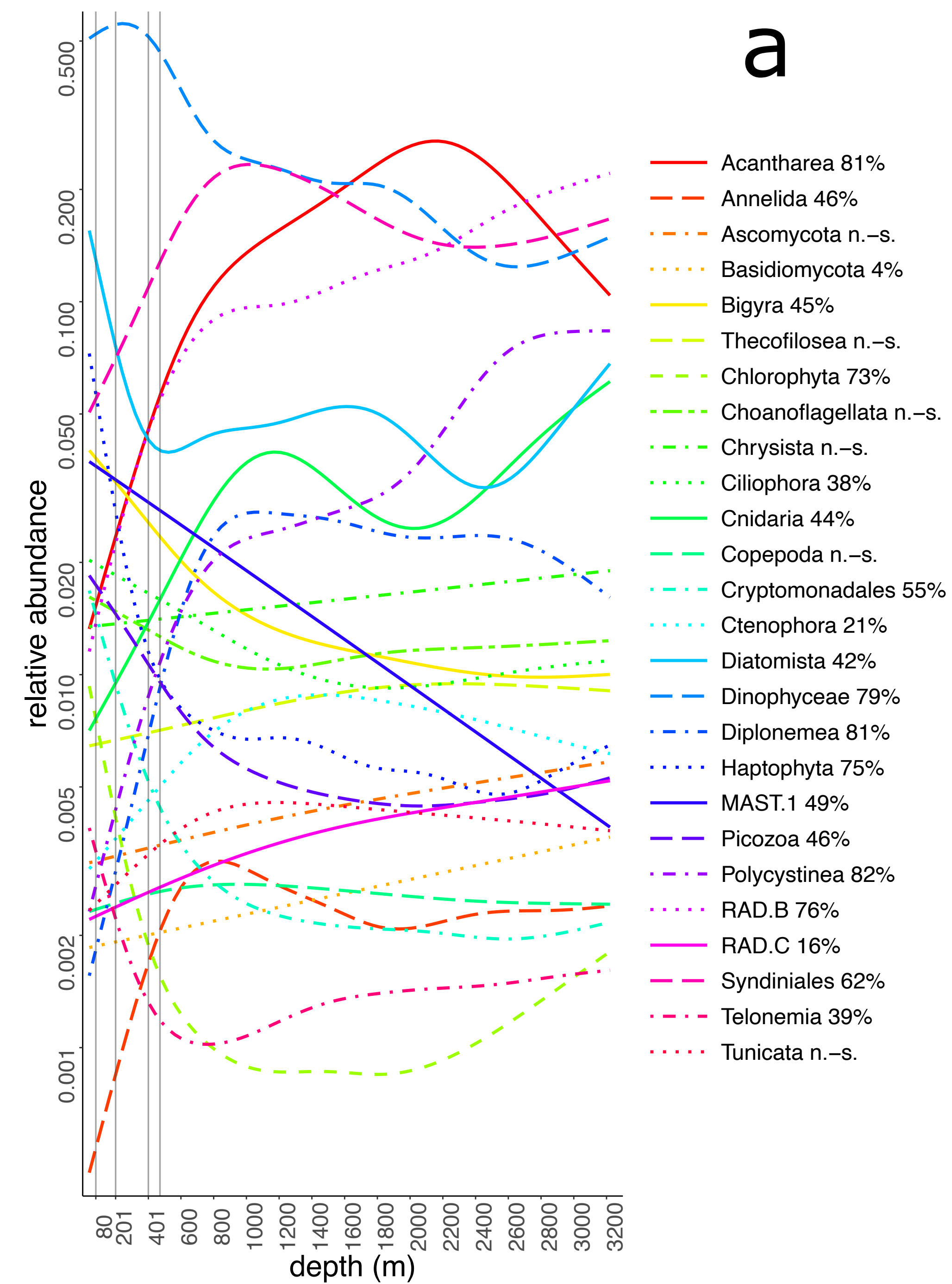


**Suppl. Fig. 4.** Square pie charts illustrating taxonomy of OTUs that were identified as “indicators” for one of five water masses (panel **a**) or one of five intervals of oxygen concentration (panel **b**) separated by the ecological boundaries (Fig. 2). Taxonomic groups are labelled and numbered according to the legend. The water masses or oxygen concentration intervals are labelled in black.

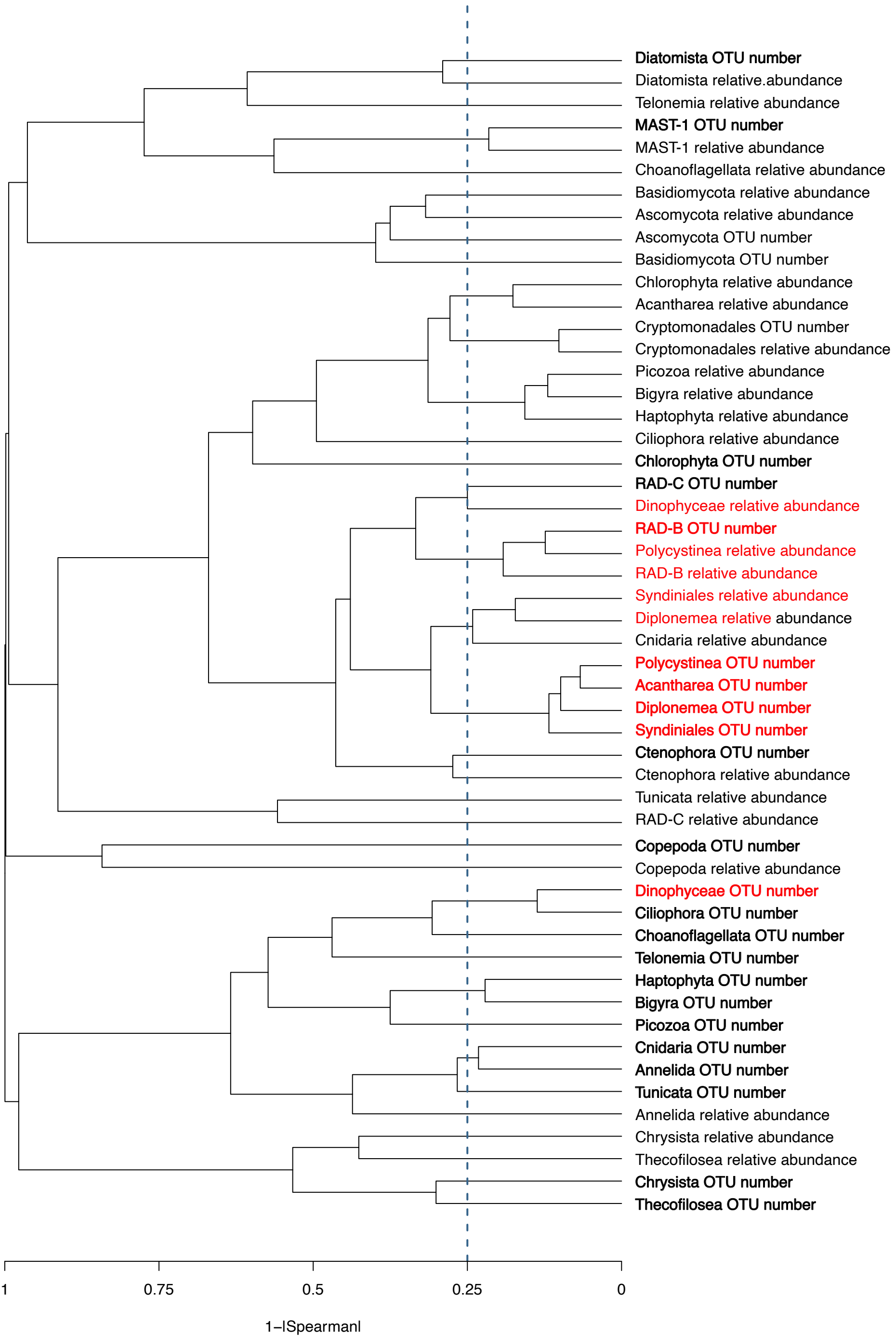




**Suppl. Fig. 5.** Distribution of 26 eukaryotic taxonomic groups across the five water masses. Relative abundance (**a**) or OTU richness (**b**) values are shown in the form of boxplots. The y-axis scales are logarithmic.

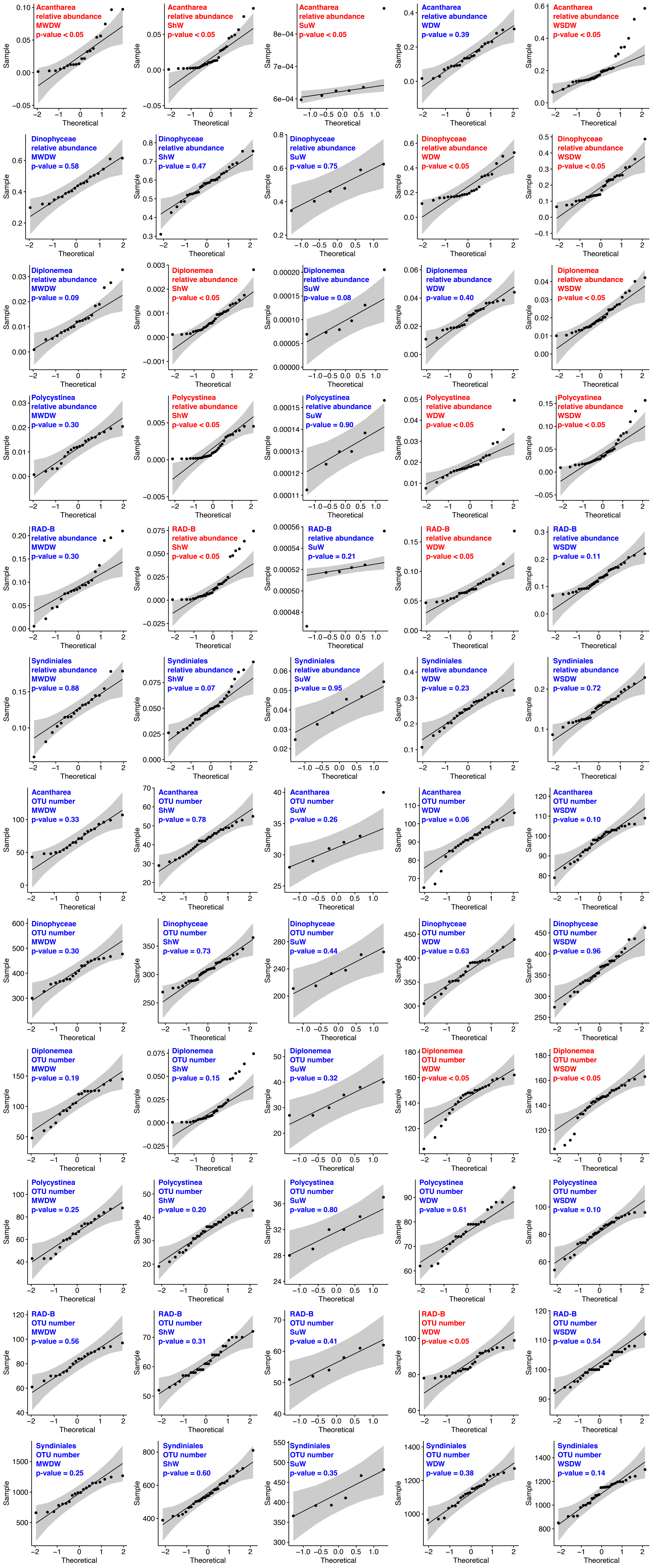


**Suppl. Fig. 6.** Plots illustrating relative abundance (**a**, **b**) or OTU richness (**c**, **d**) of 26 eukaryotic taxonomic groups changing with depth (**a**, **c**) or oxygen concentration (**b**, **d**) in the Western Weddell Sea. Only trend lines calculated using the GAM approach are shown along with percentage of variance explained. Confidence intervals for GAMs and individual data points are not shown for simplicity. The y-axes scales are logarithmic. Oxygen concentration or depth values identified as ecological boundary points are marked with vertical grey lines.



**Suppl. Fig. 7.** A dendrogram visualizing a matrix of pairwise Spearman correlation coefficients ( $1 - |\text{Spearman coefficient}|$ ) for relative abundance and OTU richness of 26 eukaryotic clades. Most important members of the deep-sea community are highlighted in red.





**Suppl. Fig. 8.** Normality test results for relative abundance values and OTU counts of six key players in the deep-sea eukaryotic community distributed across five water masses. Quantile-Quantile plots, confidence intervals and p-values of the Shapiro-Wilk test are shown.